Fuel 225 (2018) 256–265

Contents lists available at ScienceDirect

Fuel

journal homepage: www.elsevier.com/locate/fuel

Full Length Article

Soot propensity by image magnification and artificial intelligence☆

Julio Pino[a], Hugo O. Garcés[b], Juan Cuevas[c], Luis E. Arias[d], Alejandro J. Rojas[d], Andrés Fuentes[a,*]

[a] Departamento de Industrias, Universidad Técnica Federico Santa María, Avenida España 1680, Valparaiso 2390123, Chile
[b] Computer Science Department, Universidad Católica de la Santísima Concepción, Alonso de Ribera 2850, Concepción 4090541, Chile
[c] School of Civil Engineering, The University of Queensland, QLD 4072, Australia
[d] Department of Electrical Engineering, Universidad de Concepción, Concepción 4070386, Chile

ARTICLE INFO

Keyword:
Combustion
Smoke point
Artificial intelligence
Image magnification
Diagnostics

ABSTRACT

This paper presents the results of two novel approaches to measure the soot propensity of a flame and their comparison with the Line of Sight Attenuation (LOSA) method. Both approaches are based on the detection of the Smoke Point Height (SPH), concept used to determine when a flame is in a sooting state. The first approach is based on the detection of morphological changes in the flame, identified through their amplification via the Eulerian Video Magnification algorithm. Results show an effective amplification of the flame geometry, allowing the visualization of variations on the flame tip unable to be detected by the naked human eye and therefore the detection of SPH. The second approach is based on the application of Artificial Intelligence models to classify flame images regarding their sooting propensity, taking advantage of the knowledge acquired from a referential data set. Both approaches provide an accurate classification when compared to the conventional method of LOSA. Furthermore, both approaches show a greater implementation potential in practical combustion devices than the conventional method of LOSA, due to their reduced hardware and technical requirements.

1. Introduction

Combustion diagnostics has always been an active research area for many scientists and engineers from different fields, such as chemistry, physics, and mechanics,among others. In this sense, several methods have been developed to obtain information about the current state of a combustion process, motivated by improving its efficiency, decreasing its environmental impact, or optimizing key process variables [1–4]. Several techniques have been developed based on flame chemiluminescence field measurements, using optical sensors such as cameras, spectrometers, photo-diode arrays, and even combinations of them [5,6,2,7]. Soot formation in the flame is related to high and undesirable particulate matter emissions to the atmosphere [8], and therefore stands as a relevant parameter to be controlled in any given combustion process. Thus, of these techniques are based on the determination of the flame's Sooting Propensity, defined as the ratio between the formation (S_{for}) and oxidation (S_{ox}) reactions occurring within the flame [9]. An example of this is the approach presented in [10] that defines the Sooting Propensity of a fuel in terms of its Smoke Point Height (SPH), that denotes the specific moment when the flame opens its tip and releases soot, as described in [11]. Additionally, this specific moment is defined as the Smoke Point. Smoke Point Height has also being found to relate a fuel's sooting tendency with other combustion-relevant parameters such as Soot Volume Fraction [12], or Heat Release Rate [9]. Unfortunately, due to the subtle nature of the changes in the flame used as study variables, the evaluation of SPH is highly subjective and uncertain. In addition, SPH analysis requires expert knowledge and large measurement times. In order to improve the quality of these results, it is necessary to incur in more complex and computationally demanding methods.

The main contribution of this work is to present two novel approaches to evaluate soot propensity based on flame images processing. The first approach is based on a flame image magnification algorithm presented in [13]. The second approach is based on the capabilities of artificial intelligence models to solve a classification problem of sooting and non-sooting flame images, under the assumption of a previously available flame images data set. These novel approaches will be benchmarked against conventional Line of Sight Attenuation measurements (LOSA).

☆ This was presented in Tenth Mediterranean Combustion Symposium, September 2017, Napoli, Italy.

* Corresponding author.
E-mail addresses: julio.pino@alumnos.usm.cl (J. Pino), hugogarces@ucsc.cl (H.O. Garcés), j.cuevas@uq.edu.au (J. Cuevas), luiarias@udec.cl (L.E. Arias), arojasn@udec.cl (A.J. Rojas), andres.fuentes@usm.cl (A. Fuentes).

https://doi.org/10.1016/j.fuel.2018.03.141
Received 20 December 2017; Received in revised form 9 March 2018; Accepted 20 March 2018

2. Materials and methods

2.1. Line of sight attenuation fundamentals

To determine the release of soot from the flame, the radially-integrated soot volume fraction β is evaluated according to the following expression (Eq. (1)) [14],

$$\beta = 2\pi\int_0^\infty f_s r dr \approx 2\pi\Delta r\sum_{i=1}^{N} f_{s,i} r_i \tag{1}$$

where $i = 0,1,...,N-1$ is a discretization index, r is the distance from the flame's symmetry axis,and $f_s(r)$ is the local soot volume fraction, determined from the spectral absorption coefficient ($\kappa_{s,\lambda}$) distribution, as presented in Eq. (2).

$$f_s = \lambda\frac{\kappa_{s,\lambda}}{C_\lambda} \tag{2}$$

In this expression, C_λ is the absorption function, determined as presented in Eq. (3),

$$C_\lambda = \frac{36\pi n_s k_s}{(n_s^2-k_s^2+2)^2+4n_s^2k_s^2} \tag{3}$$

where n_s and k_s are the real and complex part of soot's refractive index, respectively. These parameters can be evaluated using Chang and Charalampopoulos correlations [15].

The spectral absorption coefficient ($\kappa_{s,\lambda}$) on the other hand, can be determined by means of its relation with the total fraction of light transmitted through the flame (τ), as presented in Eq. (4) [9,16,17],

$$-ln(\tau_\lambda) = 2\int_y^{R_f}\frac{\kappa_{\lambda(r)}}{\sqrt{r^2-y^2}}dr \tag{4}$$

The total fraction of light τ is determined through the LOSA measurements [18]. In synthesis, once τ is retrieved from the LOSA measurements, κ_λ is evaluated from Eq. (4). The parameter C_λ is obtained from Eq. (3), and along with κ_λ allows to calculate f_s from Eq. (2). Finally, with f_s, β is obtained from Eq. (1).

Furthermore, in order to compare the integrated soot volume fraction for different fuel flows, the vertical coordinate z was non-dimensionalized according to Eq. (5) [14]:

$$\eta = \frac{z\mathscr{D}}{\dot{V}} \tag{5}$$

where $\dot{V}$ is the volumetric fuel flow rate in sccm, and $\mathscr{D}$ is the diffusion coefficient. A value of $\mathscr{D} = 0.156\ cm^2/s$ was considered [14].

2.2. Eulerian Video Magnification fundamentals

Eulerian Video Magnification (EVM) [13] is a method to amplify subtle movement variations in an arbitrary object measured with a digital camera, usually imperceptible to the naked human eye. Fig. 1 shows a schematic of the image processing by EVM. First, EVM receives a digital video as the input and decomposes it into different spatial frequency bands. Afterward, a temporal processing is realized on each spatial band. Temporal processing consider the value of a pixel as a time series containing the desire amplified movement and noise, then it is necessary to apply a narrow bandpass filter to extract the frequency bands of interest and attenuates the noise. The bandpass filter central frequency parameter is selected, in order to suits the observed phenomenon and retaining only the desired amplified motions of the flame, which depends on the flame flickering. Finally, the extracted bands are amplified by a user-defined magnification factor α and then incorporated into the original input, generating a video-enhanced sequence of the moving object analyzed. EVM will be used to evaluate the SPH from a series of images of flames, determining the moment at which the flame tip opens and starts to release soot. The main steps that are comprehended in this approach are presented next.

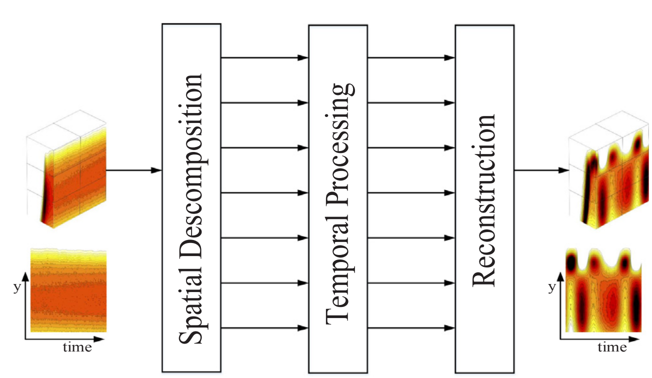

Fig. 1. Overview of the Eulerian Video Magnification framework.

2.2.1. Step 1: spatial decomposition

The first step consists of the enhancement of the contours of the image. This process can be summarized as a reduction and expansion of the image. Firstly, a flame image reduction it is obtained by applying a Gaussian pyramid according to Eq. (6), where $w(m,n)$ is the weighted average function and $g_l(i,j)$ is the value of the level l in the position (i,j) in the Gaussian Pyramid. Secondly, the image expansion is calculated based on Eq. (7), where the value $L_l(i,j)$ corresponds to the level l in the pixel (i,j) on the Laplacian Pyramid. Fig. 2a shows a schematic of the Gaussian pyramid pixels averaging, and Fig. 2b shows the results of the application of this Gaussian pyramid. Finally, Fig. 2c shows the result of image enhancement process, where the flame image contours are amplified.

$$g_l(i,j) = \sum_{m=-2}^{2}\sum_{n=-2}^{2} w(m,n)g_{l-1}(2i+m,2j+n) \tag{6}$$

$$L_l(i,j) = g_l(i,j)-EXPAND(g_{l+1}(i,j)) \tag{7}$$

2.2.2. Step 2: temporal processing

In EVM, movement is approximated through a first order Taylor series according to Eq. (8) [13], where $L(x,t)$ is the intensity of the image in the position x at the time t. Then, an estimated amplified motion $\hat{L}_l(x,t)$ is obtained by amplifying the movement variation associated to the derivative term in Eq. (8), as presented in Eq. (9) [13]:

$$L_l(x,t) \approx f(x) + \delta(t)\frac{\Delta f(x)}{\Delta x} \tag{8}$$

$$\hat{L}_l(x,t) \approx f(x) + [1+\alpha]\delta(t)\frac{\Delta f(x)}{\Delta x} \tag{9}$$

where $f(x) = L_l(x,0)$ and α is a magnification parameter between [10 and 20].

The bandpass filter selection in EVM is application dependent [13], but for motion amplification as in the case of the flame images, a broad bandpass is preferred [13]. A simple approach is given by a bandpass IIR filter, which is obtained by the use of two first-order lowpass IIR filters with cut-off frequencies w_{low} and w_{high} according to the minimum and maximum feasible flame flickering. The relation between the coefficients a_1 and b_0 of a first-order lowpass IIR filter and its filtered output $\Psi(k)$ is defined in Eq. (10), where $\varepsilon(k)$ is the original time series representing the pixel temporal response.

$$\Psi(k) = a_1\cdot\Psi(k-1) + b_0\cdot\varepsilon(k) \tag{10}$$

2.2.3. Step 3: reconstruction

Finally, the enhanced image is obtained by means of concatenation of the spatial decomposition obtained from step 1 and the motion amplification obtained from step 2. Fig. 3 presents an example of this